

# Performance Comparison of a Three Phase AC to Three Phase AC Matrix Converter using Different Carrier based Switching Algorithms

Dr. Narayanaswamy P R Iyer\*,  
\*Electrical and Electronics Consultant ,  
59, Oakhill Drive, Castle Hill,  
NSW-2154, Ausatrlia.

Prof. Chem V Nayar†#  
†Emeritus Professor, School of ECE,  
Curtin University of Technology, Perth,  
WA, Australia.  
#Managing Director,  
Regenpower Pty. Ltd., Perth, WA, Australia.

**Abstract** - Recently considerable interest is shown in the use of Matrix Converters for industrial drive applications. Since the inception, several carrier based modulation schemes have been proposed for Matrix Converters. The operation and control methodology of Matrix Converters is complex. This paper examines the various modulation schemes for three phase AC to three phase AC matrix converters starting from the Venturini and optimum Venturini algorithm to the recently developed Sunter-Clare and Ned Mohan algorithm, by modelling technique. The simulation is carried out using PSCAD for a given input, output, carrier switching frequency and modulation index. The simulation results are presented and compared. The relative merits of each algorithm from the point of view of high Peak Fundamental value and low Total Harmonic Distortion for the line to neutral, line to line voltages and input current are analysed and tabulated.

**Keywords:** Matrix Converter, AC to AC Converter, Carrier based algorithms, PSCAD model, Simulation.

## 1 INTRODUCTION

Recently considerable interest is shown in the development of AC to AC converters also known as “Matrix Converters” for Adjustable Speed Drive applications [1-4]. Matrix converters are essentially forced commutated cycloconverters consisting of a matrix of bidirectional switches such that there is a switch for each possible connection between the input and output lines. For a three phase AC to three phase AC matrix converter there are nine bidirectional semiconductor switches. A three phase AC to three phase AC matrix converter is shown in Fig. 1. While operating the Matrix Converter, two essential points must be remembered. The three or any two combination of the bidirectional switches in any one output phase should not be closed at the same instant of time [1-4]. Referring to Fig. 1, if any two or all of switches SAa, SBa and SCa are closed simultaneously, the input lines are short circuited causing dangerous short circuit currents through the bidirectional switches. Similarly with inductive loads all the three bidirectional switches connected to an output phase should not be open simultaneously [1-4]. One switch at least in any output phase must remain closed. Matrix converter directly converts the AC input voltage at any given frequency to AC output voltage with arbitrary amplitude at any unrestricted frequency without the need for a dc link capacitor storage element at the input side. Sinusoidal input and output currents can be obtained

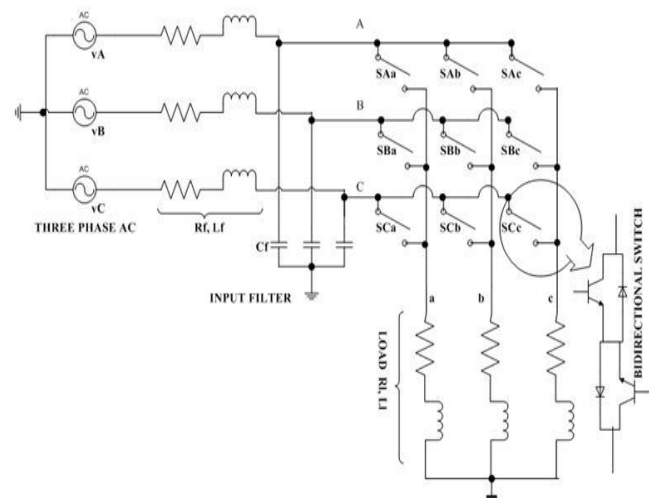


Fig. 1 MATRIX CONVERTER

with unity power factor for any load. It has regeneration capability [1-4]. One limitation of the matrix converter is that the maximum output voltage available is limited to 86.6 % of the input voltage in the linear modulation range.

The real development of the matrix converter starts with the work of Venturini and Alesina who proposed a mathematical analysis and introduced the Low-Frequency Modulation Matrix concept to describe the low frequency behavior of the matrix converter [5-7]. In this, the output voltages are obtained by multiplication of the modulation matrix or transfer matrix with the input voltages.

The 3 X 3 matrix converter shown in Fig.1 connects the three phase AC source to the three phase load. The switching Function for a 3 X 3 matrix converter can be defined as follows:

$$S_{Kj} = \begin{cases} 1 & \text{when } S_{Kj} \text{ is closed} \\ 0 & \text{when } S_{Kj} \text{ is open} \end{cases} \quad (1)$$

$K \in A, B, C$  and  $j \in a, b, c$

The above constraint can be expressed in the following form:

$$S_{Aj} + S_{Bj} + S_{Cj} = 1 \quad (2)$$

$j \in a, b, c$

With the above restrictions a 3 X 3 matrix converter has 27 possible switching states [8].

The mathematical expression that represents the operation of a three phase AC to AC Matrix Converter (MC) can be expressed as follows:

$$\begin{bmatrix} v_a(t) \\ v_b(t) \\ v_c(t) \end{bmatrix} = \begin{bmatrix} S_{Aa}(t) & S_{Ba}(t) & S_{Ca}(t) \\ S_{Ab}(t) & S_{Bb}(t) & S_{Cb}(t) \\ S_{Ac}(t) & S_{Bc}(t) & S_{Cc}(t) \end{bmatrix} * \begin{bmatrix} v_A(t) \\ v_B(t) \\ v_C(t) \end{bmatrix} \quad (3)$$

$$\begin{bmatrix} i_A(t) \\ i_B(t) \\ i_C(t) \end{bmatrix} = \begin{bmatrix} S_{Aa}(t) & S_{Ba}(t) & S_{Ca}(t) \\ S_{Ab}(t) & S_{Bb}(t) & S_{Cb}(t) \\ S_{Ac}(t) & S_{Bc}(t) & S_{Cc}(t) \end{bmatrix}^T * \begin{bmatrix} i_a(t) \\ i_b(t) \\ i_c(t) \end{bmatrix} \quad (4)$$

where  $v_a$ ,  $v_b$  and  $v_c$  and  $i_A$ ,  $i_B$  and  $i_C$  are the output voltages and input currents respectively. To determine the behavior of the MC at output frequencies well below the switching frequency, a modulation duty cycle can be defined for each switch. The modulation duty cycle  $M_{Kj}$  for the switch  $S_{Kj}$  in Fig.1 is defined as in equation 5 below:

$$M_{Kj} = \frac{t_{Kj}}{T_s} \quad (5)$$

$K \in \{A, B, C\}$  and  $j \in \{a, b, c\}$

where  $t_{Kj}$  is the on time for the switch  $S_{Kj}$  between input phase  $K \in \{A, B, C\}$  and  $j \in \{a, b, c\}$  and  $T_s$  is the period of the PWM switching signal or sampling period. In terms of the modulation duty cycle, equations 2, 3 and 4 can be rewritten as given below:

$$\begin{bmatrix} v_a(t) \\ v_b(t) \\ v_c(t) \end{bmatrix} = \begin{bmatrix} M_{Aa}(t) & M_{Ba}(t) & M_{Ca}(t) \\ M_{Ab}(t) & M_{Bb}(t) & M_{Cb}(t) \\ M_{Ac}(t) & M_{Bc}(t) & M_{Cc}(t) \end{bmatrix} * \begin{bmatrix} v_A(t) \\ v_B(t) \\ v_C(t) \end{bmatrix} \quad (6)$$

$$\begin{bmatrix} i_A(t) \\ i_B(t) \\ i_C(t) \end{bmatrix} = \begin{bmatrix} M_{Aa}(t) & M_{Ba}(t) & M_{Ca}(t) \\ M_{Ab}(t) & M_{Bb}(t) & M_{Cb}(t) \\ M_{Ac}(t) & M_{Bc}(t) & M_{Cc}(t) \end{bmatrix}^T * \begin{bmatrix} i_a(t) \\ i_b(t) \\ i_c(t) \end{bmatrix} \quad (7)$$

$$M_{Aj} + M_{Bj} + M_{Cj} = 1, j \in \{a, b, c\} \quad (8)$$

## 2. ALGORITHMS FOR MATRIX CONVERTERS

The modulation problem encountered in matrix converters can be expressed as follows:

Let the input and output voltages be expressed as in equation 9 and 10 below:

$$v_i = \begin{bmatrix} v_A \\ v_B \\ v_C \end{bmatrix} = V_{im} * \begin{bmatrix} \cos(\omega_i t) \\ \cos(\omega_i t + \frac{4\pi}{3}) \\ \cos(\omega_i t + \frac{2\pi}{3}) \end{bmatrix} \quad (9)$$

$$v_o = \begin{bmatrix} v_a \\ v_b \\ v_c \end{bmatrix} = q * V_{im} * \begin{bmatrix} \cos(\omega_o t) \\ \cos(\omega_o t + \frac{4\pi}{3}) \\ \cos(\omega_o t + \frac{2\pi}{3}) \end{bmatrix} \quad (10)$$

where  $q$  is the voltage transfer ratio.

### 2.1 Venturini and Optimum Venturini Modulation Algorithms

The first method of Venturini is the derivation of the transfer matrix by directly solving equations 6, 9 and 10 using the constraint in equation 8 [1-2]. Calculating switching times directly from this transfer matrix is difficult for practical implementation [1-2]. For unity input displacement factor a convenient method of expressing the modulation function is given below:

$$M_{Kj} = \frac{t_{Kj}}{T_s} = \left[ \frac{1}{3} + \frac{2v_K \cdot v_j}{3 \cdot V_{im}^2} \right] \quad (11)$$

for  $K = A, B, C$  and  $j = a, b, c$

This method is of little significance because of the 50 % voltage ratio limitation [1-2].

Venturini's optimum method employs common mode addition technique defined in equation 12 below:

$$v_o = \begin{bmatrix} v_a \\ v_b \\ v_c \end{bmatrix} = q * V_{im} * \begin{bmatrix} \cos(\omega_o t) - \frac{1}{6} * \cos(3\omega_o t) + \frac{1}{2\sqrt{3}} * \cos(3\omega_i t) \\ \cos(\omega_o t + \frac{4\pi}{3}) - \frac{1}{6} * \cos(3\omega_o t) + \frac{1}{2\sqrt{3}} * \cos(3\omega_i t) \\ \cos(\omega_o t + \frac{2\pi}{3}) - \frac{1}{6} * \cos(3\omega_o t) + \frac{1}{2\sqrt{3}} * \cos(3\omega_i t) \end{bmatrix} \quad (12)$$

Using  $v_o$  defined as in equation 12, for unity input displacement factor, the modulation function can be expressed as in equation 13 below:

$$M_{Kj} = \frac{t_{Kj}}{T_s} = \left[ \frac{1}{3} + \frac{2v_K \cdot v_j}{3 \cdot V_{im}^2} + \frac{4q}{9\sqrt{3}} * \sin(\omega_i t + \beta_K) * \sin(3\omega_i t) \right] \quad (13)$$

for  $K = A, B, C$  and  $j = a, b, c$  and  $\beta_K = 0, \frac{2\pi}{3}, \frac{4\pi}{3}$  respectively.

### 2.2 Sunter-Clare modulation algorithm

The Venturini algorithm approach is unsuitable for closed loop applications where it is required to calculate the duty cycle every sampling period to achieve voltage control in which output frequency is continuously varying with time [10]. To overcome this problem the approach taken is to measure the input voltage at every sampling period and to determine voltage vector magnitude and ratio and position directly [9-11]. A simplified version of Venturini algorithm is defined in terms of

the three phase input and output at each sampling instant [9-11]. This allows the demand voltage ratio, output voltage magnitude and angle to be updated at every sampling period which is a requirement for closed loop control [9-11].

For the real time implementation of the proposed modulation algorithm, it is required to measure any two of three line to line input voltages. Then  $V_{im}$  and  $\omega_i.t$  are calculated as give below [10-11].

$$V_{im}^2 = \frac{4}{9} \cdot [v_{AB}^2 + v_{BC}^2 + v_{AB} \cdot v_{BC}] \quad (14)$$

$$\omega_i.t = \arctan \left[ \frac{V_{BC}}{\sqrt{3} \cdot \left( \frac{2 \cdot V_{AB}}{3} + \frac{V_{BC}}{3} \right)} \right] \quad (15)$$

where  $v_{AB}$ ,  $v_{BC}$  are the input line voltages.

The target output peak voltage and position are calculated as follows:

$$V_{om}^2 = (2/3) \cdot [V_a^2 + V_b^2 + V_c^2] \quad (16)$$

$$\omega_o.t = \arctan[(V_b - V_c) / (\sqrt{3} \cdot V_a)] \quad (17)$$

where  $V_a$ ,  $V_b$  and  $V_c$  are the target phase output voltages. In a closed loop system such as a field oriented or a vector controlled drive system, the voltage magnitude and angle may be direct outputs of the control loop. Then the voltage ratio is calculated as follows:

$$q = \sqrt{\frac{V_{om}^2}{V_{im}^2}} \quad (18)$$

where  $q$  is the desired voltage ratio and  $V_{im}$  is the peak input voltage. The triple harmonic terms are found using the following equations:

$$K_{31} = \frac{2q}{9q_m} \cdot \sin(\omega_i t) * \sin(3\omega_i t) \quad (19)$$

$$K_{32} = \frac{2q}{9q_m} \cdot \sin\left(\omega_i t - \frac{2\pi}{3}\right) \cdot \sin(3\omega_i t) \quad (20)$$

$$K_{33} = -\sqrt{V_{om}^2} \cdot \left[ \frac{1}{6} \cdot \cos(3\omega_o t) - \frac{1}{4q_m} \cdot \cos(3\omega_i t) \right] \quad (21)$$

where  $q_m$  is the maximum voltage transfer ratio which is 0.866. Then the three modulation functions for output phase a are given as follows.

$$M_{Aa} = \frac{1}{3} + k_{31} + \frac{2}{3V_{im}^2} \cdot (v_a + k_{33}) \cdot \left( \frac{2v_{AB}}{3} + \frac{v_{BC}}{3} \right) \quad (22)$$

$$M_{Ba} = \frac{1}{3} + k_{32} + \frac{2}{3V_{im}^2} \cdot (v_a + k_{33}) \cdot \left( \frac{v_{BC}}{3} - \frac{v_{AB}}{3} \right) \quad (23)$$

$$M_{Ca} = 1 - (M_{Aa} + M_{Ba}) \quad (24)$$

The modulation functions for the other two output phases b and c are obtained by replacing  $v_a$  with  $v_b$  and  $v_c$  in equations 22 and 23. The modulation functions have third harmonic components at the input and output frequencies added to them to produce output voltage  $V_o$ . This is a requirement for getting maximum possible voltage ratio. The three phase output voltages and input currents can be defined in terms of modulation functions as given in equations 6 to 8.

### 2.3 Ned Mohan modulation algorithm

A novel carrier-based modulation scheme is proposed by Ned Mohan which requires no sector information and look-up table to calculate duty ratios, with output voltage amplitude 0.866 times that of the input voltage and the input power factor controllable [12-14]. This algorithm is briefly explained below:

Let the three phase input voltages,  $v_i = [V_A \ V_B \ V_C]^T$  be defined as in equation 9 and the corresponding output phase voltages be defined as in equation 6 above. The duty ratios be chosen such that the output voltages are independent of the input frequency. This is possible by considering the input voltages in stationary reference frame and the output voltages in synchronous reference frame. Hence  $M_{Aa}$ ,  $M_{Ba}$  and  $M_{Ca}$  are chosen as given in equation 25 below:

$$M_{Ka} = k_a * \cos(\omega_i t - \phi_i - \gamma) \quad (25)$$

Using equation 6, 9 and 25 and simplifying, the output voltage equation  $v_a$  for Phase a reduces to the following:

$$v_a = \frac{3}{2} * k_a * \cos(\phi_i) \quad (26)$$

Equation 26 shows that the output phase voltage  $v_a$  is independent of the input frequency but dependent only on the amplitude of the input voltage. The modulation index  $k_a$  is a function of the output angular frequency  $\omega_o$  as defined below:

$$k_j = k * \cos(\omega_o t - \gamma) \quad (27)$$

Using equations 26 and 27, the output phase voltage  $v_a$  simplifies to the following:

$$v_a = \left[ \frac{3}{2} \cdot k \cdot V_{im} \cdot \cos(\phi_i) * \cos(\omega_o t) \right] \quad (28)$$

From equation 25 and 27, it is clear that the duty-ratios of the switches takes negative values. But the requirement is that the duty ratios of the switches must lie in the range 0 to 1. This is made possible by adding offset duty ratios to the existing duty ratios. Thus absolute values of duty ratios are added. The offset duty ratio is defined by equation 29 below:

$$D_K(t) = |k_a * \cos(\omega_i t - \phi_i - \gamma)| \quad (29)$$

Thus the new duty ratios are defined below:

$$M_{Ka} = D_K(t) + k_a * \cos(\omega_i t - \phi_i - \gamma) \quad (30)$$

Using equation 29 in 30, in order that the new duty ratio in 30 lies in the range 0 to 1, the following inequality should be satisfied:

$$0 < 2 \cdot |k_a| = 2 \cdot k < 1 \quad (31)$$

Thus the maximum value of  $k_a$  and  $k$  can be 0.5. Using this value, the offset duty ratios are chosen as given below:

$$D_K(t) = |0.5 \cdot \cos(\omega_i t - \phi_i - \gamma)| \quad (32)$$

To utilize the input voltage capability to the full extend, additional common mode voltage term is added which gives the new modulation index as given below:

$$M_{Ka} = D_K(t) + [k_a - \{\max(k_a, k_b, k_c) + \min(k_a, k_b, k_c)\} / 2] \cdot \cos(\omega_i \cdot t - \phi_i - \gamma) \quad (33)$$

In equations 25 to 33, the symbols  $K$ ,  $j$  and  $\gamma$  are defined as follows:

$$K = A, B, C; j = a, b, c \text{ and } \gamma = 0, \frac{2\pi}{3}, \frac{4\pi}{3} \text{ respectively.}$$

To calculate input power factor, the input current is represented as a function of duty ratios and output currents, as defined in equation 7 above. Hence the input current in phase A can be expressed as follows:

$$i_A = (k_a \cdot i_a + k_b \cdot i_b + k_c \cdot i_c) \cdot \cos(\omega_i t - \phi_i) \quad (34)$$

In equation 34, the modulation index and output currents are at output frequency. Equation 34 simplifies to the following:

$$i_A = \left(\frac{3}{2} \cdot k \cdot I_o \cdot \cos(\phi_o)\right) \cdot \cos(\omega_i t - \phi_i) \quad (35)$$

where  $I_o$  is the amplitude of the output current and  $\phi_o$  is the output power factor angle.

Comparing equation 35 with the input phase voltage  $v_A$ , it is seen that the input current lags the input phase voltage by an angle of  $\phi_i$ . Thus  $\phi_i$  is chosen to be zero for unity input power factor operation. Also comparison of equation 28 with equation 10 reveals the following relationship with  $q$ :

$$q = \left[\frac{3}{2} \cdot k \cdot \cos(\phi_i)\right] \quad (36)$$

### 3. MODEL DEVELOPMENT

To study the performance of the three phase matrix converter using all the above algorithms, a model was developed for each algorithm, using PSCAD [15]. The data used for all the algorithms are given in Table I.

TABLE I: PARAMETERS

Sl.No.	Parameter	Value	Unit
1)	RMS Line to Neutral Input Voltage	220	Volts
2)	Input Frequency	50	Hz
3)	Output Frequency	50	Hz
4)	Modulation Index $q / k$	0.4 / 0.26667	--
5)	Carrier Switching Frequency	5	kHz
6)	Output RLC Filter	10, 2e-3, 0.50712e-6	$\Omega, H, F$
7)	R-L Load	50, 0.5	$\Omega, H$

In Table 1, the value of  $q$  and saw-tooth carrier are used for for Venturini, Optimum Venturini and Sunter-Clare algorithm where as the value of  $k$  and triangle carrier are used for Ned Mohan algorithm.

### 4. SIMULATION RESULTS

For the Venturini and the optimum Venturini algorithm, equation 11 and equations 12 with 13 were used to determine the duty cycle for the nine bidirectional switches, for the former and the later algorithm respectively. For the Sunter-Clare algorithm, equations 22 to 24 and for the Ned Mohan algorithm equation 33 were used to determine the duty cycle for the nine bidirectional switches. In the case of Ned Mohan algorithm, the  $k$  value was determined for a  $q$  value of 0.4 using equation 36 assuming unity input power factor [16-17].

The simulation results relating to Venturini, Optimum Venturini, Sunter-Clare and Ned Mohan algorithm are shown in Fig.2, 3, 4 and 5 respectively. These results are tabulated in Table II.

### 5. DISCUSSION OF RESULTS

From the simulation results shown in Table II, it is seen that the peak fundamental value of line to neutral voltage is highest for Optimum Venturini and lowest for Ned Mohan

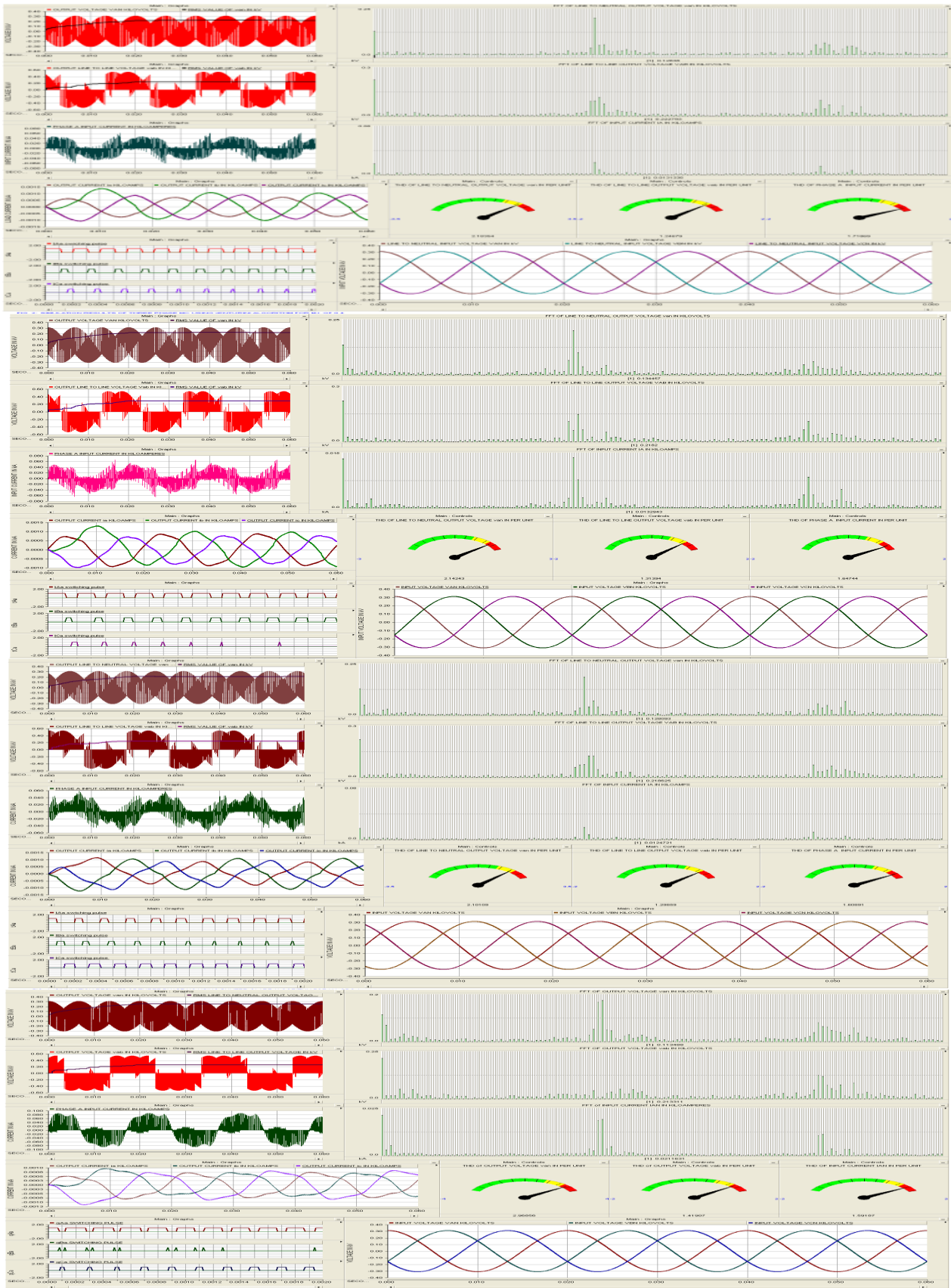


Fig. 2, 3, 4 & 5(T to B): PSCAD Simulation results: Venturini, Optimum Venturini, Senter-Clare and Ned Mohan Modulation Algorithms

Table II Simulation Results

Sl.No.	Name of Algorithm	Parameters	Peak Fundamental Value			Total Harmonic Distortion		
			Line to Neutral Voltage (V)	Line to Line Voltage (V)	Input Current (A)	Line to Neutral Voltage (p.u.)	Line to Line Voltage (p.u.)	Input Current (p.u.)
1)	Venturini	Table 1	128.38	222.79	13.13	2.183	1.246	1.718
2)	Optimum Venturini	Table 1	134.45	218.2	13.29	2.142	1.313	1.647
3)	Sunter-Clare	Table 1	128.09	218.62	12.47	2.101	1.298	1.608
4)	Ned Mohan	Table 1	113.48	213.31	21.16	2.968	1.419	1.591

algorithm. For Line to Line voltage peak fundamental Sunter-Clare algorithm gives the highest value and Ned Mohan algorithm gives the lowest value. The Input Current peak fundamental is highest for Ned Mohan algorithm and lowest for Sunter-Clare algorithm. The THD of line to neutral voltage, line to line voltage and input current in order is the lowest for Sunter-Clare, Venturini and Ned Mohan algorithm respectively. The linear range for modulation index for Venturini algorithm is 0 to 0.5 and for Optimum Venturini and Sunter-Clare algorithm this value is in the range 0 to 0.866. For Ned Mohan algorithm, the linear modulation range is from 0 to 0.577. The modulation index is in the linear range for all the above algorithms and there for the predicted performance will yield only similar results as long as the modulation index is within the linear range. The predicted performance here has only minor differences compared to that without output filter [16].

## 6. CONCLUSIONS

Four carrier based algorithms for switching three phase AC to three phase AC Matrix Converter have been studied in detail by modeling using PSCAD. The relative merits of each algorithm from the point of view of high peak fundamental value and low THD have been examined and tabulated. The algorithm number 3 and 4 of Table 2 are recently proposed. The modulation index is within the linear range for all the four algorithms and hence the predicted performance is valid for all values of modulation index within the linear modulation range.

## REFERENCES

- [1] Patrick Wheeler, Jose Rodriguez, J.C. Clare, Lee Empringham and A. Weinstein: "Matrix Converters – A Technology Review", IEEE Transactions on Industrial Electronics, Vol. 49, No.2, April 2002, pp. 276 – 288.
- [2] Patrick Wheeler, J. Clare, Lee Empringham, M. Apap and M. Bland: "Matrix Converters", Power Engineering Journal, December 2002, pp. 273 – 282.
- [3] Sedat Sunter and J.C. Clare: "Development of a Matrix Converter Induction Motor Drive", IEEE MELECON, Antalya, 1994, pp. 833 – 836.
- [4] Sedat Sunter and J.C. Clare: "A True Four Quadrant Matrix Converter Induction Motor Drive with Servo Performance", IEEE PESC, Italy, 1996, pp. 146 – 151.
- [5] A. Alesina and M.G.B. Venturini: "Solid State Power Conversion: A Fourier Analysis Approach to Generalized Transformer Synthesis", IEEE Transactions on Circuits and Systems, Vol. CAS-28, No.4, April 1981, pp. 319 – 330.
- [6] A. Alesina and M. Venturini: "Intrinsic Amplitude Limits and Optimum Design of 9-Switches Direct PWM AC-AC Converters", IEEE-PESC, 1988, pp. 1284 – 1291.
- [7] A. Alesina and M. Venturini: "Analysis and Design of Optimum Amplitude Nine-Switch Direct AC-AC Converters", IEEE Transactions on Power Electronics, Vol.4, January 1989, pp. 101 – 112.
- [8] L. Huber and D. Borojovic: "Space Vector Modulated Three-Phase to Three-Phase Matrix Converter with Input Power Factor Correction", IEEE Transactions on Industry Applications, Vol.31, No.6, November/December 1995, pp. 1234 -1245.
- [9] S. Sunter and J.C. Clare: "Feedforward Indirect Vector Control of a Matrix Converter-fed Induction Motor Drive", The International Journal for Computation and Mathematics in Electrical and Electronic Engineering, Vol. 19, No.4, 2000, pp. 974 – 986.
- [10] S. Sunter, H. Altun and J.C. Clare: "A Control Technique for Compensating the Effects of Input Voltage variations on Matrix Converter Modulation Algorithms", Electric Power Components and Systems, Taylor and Francis, Vol. 30, 2002, pp. 807 – 822.
- [11] H. Altun and S. Sunter: "Matrix Converter Induction Motor Drive: Modeling, Simulation and Control", Electrical Engineering, Vol. 86, 2003, pp. 25 – 33.
- [12] K.K. Mohapatra, P. Jose, A. Drolia, G. Aggarwal, S. Thuta and Ned Mohan: "A Novel Carrier-Based PWM Scheme for Matrix Converters that is Easy to Implement", IEEE-PESC, 2005, pp. 2410 – 2414.
- [13] T. Sathish, K.K. Mohapatra and Ned Mohan: "Steady State Over-Modulation of Matrix Converter Using Simplified Carrier Based Control", IEEE-IECON, 2007, pp. 1817 – 1822.
- [14] S. Thuta, K.K. Mohapatra and Ned Mohan: "Matrix Converter Over-Modulation Using Carrier-Based Control: Maximizing the Voltage Transfer Ratio", IEEE-PESC, 2008, pp. 1727 – 1733.
- [15] Manitoba HVDC Research Centre: "PSCAD v4.2.1", 2006.
- [16] Narayanaswamy. P.R. Iyer: "Carrier Based Modulation Technique for Three Phase Matrix Converters – State of the Art Progress", IEEE-SIBIRCON-2010, Listvyanka, Russia, July 11-15, 2010, pp. 659 - 664.
- [17] Narayanaswamy P R Iyer: "Modelling, Simulation and Real time Implementation of A Three Phase AC to AC Matrix Converter", Ph.D. thesis, Curtin University of Technology, Perth, WA, Australia, Ch.3, Ch.4 and Ch.14, February 2012.